AIP Applied Physics Letters

Surface phase-matched harmonic enhancement in a bulk anomalous dispersion medium

Huaijin Ren, Xuewei Deng, Yuanlin Zheng, Ning An, and Xianfeng Chen

Citation: Appl. Phys. Lett. **103**, 021110 (2013); doi: 10.1063/1.4813624
View online: http://dx.doi.org/10.1063/1.4813624
View Table of Contents: http://apl.aip.org/resource/1/APPLAB/v103/i2
Published by the AIP Publishing LLC.

APPLIED PHYSICS LETTERS **103**, 021110 (2013)

Surface phase-matched harmonic enhancement in a bulk anomalous dispersion medium

Huaijin Ren,[1] Xuewei Deng,[2,a)] Yuanlin Zheng,[1] Ning An,[1] and Xianfeng Chen[1,b)]
[1]*Department of Physics, Key Laboratory for Laser Plasmas (Ministry of Education), Shanghai Jiao Tong University, 800 Dongchuan Road, Shanghai 200240, China*
[2]*Laser Fusion Research Center, China Academy of Engineering Physics, Mianyang, Sichuan 621900, China*

(Received 3 April 2013; accepted 26 June 2013; published online 10 July 2013)

Scattering second harmonic ring could be observed in a bulk nonlinear medium with anomalous dispersion, whose generation is derived from complete phase matching of the incident light and the scattering light. By this specific phase matching under anomalous dispersion condition, we took advantage of total internal reflection, and realized high efficiency second harmonic output to gain a single pass conversion efficiency of up to 14.8% by only once reflection. It may suggest potential applications in micro-structures, such as micro cavities and waveguides. © *2013 AIP Publishing LLC*. [http://dx.doi.org/10.1063/1.4813624]

Frequency conversion is an effective means of generating coherent light at frequencies where lasers perform poorly or are unavailable. Traditional efficient frequency conversion methods include birefringence phase matching (BPM) by precisely controlling the angular orientation of the crystal and temperature to find the position of $2k_1 = k_2$; and quasi-phase-matching (QPM),[1] which uses the spatially periodic modulation of the second order nonlinearity to compensate for the phase mismatch ($k_2 = 2k_1 + \Delta k$). In addition to these two main methods, other efficient frequency conversion processes also have been studied. For example, conical second-harmonic (SH) beams can be generated by the incident and scattering lights in a $\chi^{(2)}$ photonic crystal where the phase mismatch is compensated by the reciprocal lattice vector;[2–4] nonlinear Cherenkov radiation is automatically longitudinal phase matched, which is more tolerant to processing parameters and produces second-harmonic light.[5–7] These techniques have been applied to optical manipulation,[8] optical measurement,[9] optical microscopy,[10] and other aspects.

Anomalous dispersion materials have features that their traditional normal dispersive counterparts do not have, which promotes our understanding of nonlinear processes in anomalous-dispersion-like environment.[11] Generally, anomalous dispersion region always corresponds to a strong absorption band, so it is difficult to carry on the nonlinear optical research in this region. However, by exploiting the birefringence of crystal, fundamental and harmonic beams can effectively simulate an anomalous-dispersion-like environment in some normally dispersion medium, and make this kind of research accessible.

In this letter, we report on an efficient frequency doubling method which exploits the specific complete phase-matching mechanism in such anomalous-dispersion-like medium. Experimentally, we observed conical second harmonic beam from a bulk crystal without any photonic microstructures, whose phenomenon could not be observed in normal dispersion medium for the limitation of its phase-matching condition. And based on this phase-matching scheme, we took advantage of total internal reflection to achieve a high efficiency second harmonic generation, the single pass conversion efficiency of which was up to 14.8% for only once reflection.

Our sample is a z-cut 5%/mol MgO:$LiNbO_3$ crystal with dimension of $3 \times 20 \times 2$ mm^3 ($x \times y \times z$). The working temperature is set at 18 °C. According to the Sellmeier equation,[12] for pump light with wavelength longer than 1023 nm, the refractive index of ordinary-polarized fundamental wave (FW) is greater than that of extraordinary-polarized second harmonic wave, which mimics anomalous dispersion. In the measurement, the output of an optical parametric amplifier (TOPAS, Coherent, Inc.) was chosen as the fundamental wave with 80 fs pulse duration and 1 kHz repetition rate. The fundamental wave was loosely focused with a beam waist of 50 μm right onto the x-surface of the sample by a 250 mm focal length lens. The output light was then projected onto a screen, which was set perpendicularly to the sample's x-axis at 5 cm away from the sample.

When the incident light was extraordinary polarized, there was only a phase-mismatched collinear second harmonic beam generated. However, when we adjusted the incident light to ordinary polarization, an extraordinary polarized conical SH emission emerged, which exhibited circular ring pattern on the screen behind the crystal, and its radius increased with the fundamental wavelength. Figure 1(a) shows the experimental conical SHG patterns with the pump wavelength ranging from 1140 nm to 1320 nm.

A comprehensive interpretation for the conical SH beam can be given by introducing an additional fundamental wave $\vec{k}'_1$. As the inset of Fig. 1(b) indicates, $\vec{k}_1$ and $\vec{k}_2$ are the wave vectors of the ordinary polarized FW and extraordinary polarized SH, respectively. The incident fundamental wave $\vec{k}_1$ propagates along the x-axis of the sample. Previous researches have found that the scattering light can provide this additional fundamental wave $\vec{k}'_1$, both in bulk crystals[13,14] and in super-lattice crystals.[2–4] The scattering is ascribed to the interaction of the incident light wave with a

a)Electronic mail: xwdeng@caep.ac.cn
b)Electronic mail: xfchen@sjtu.edu.cn

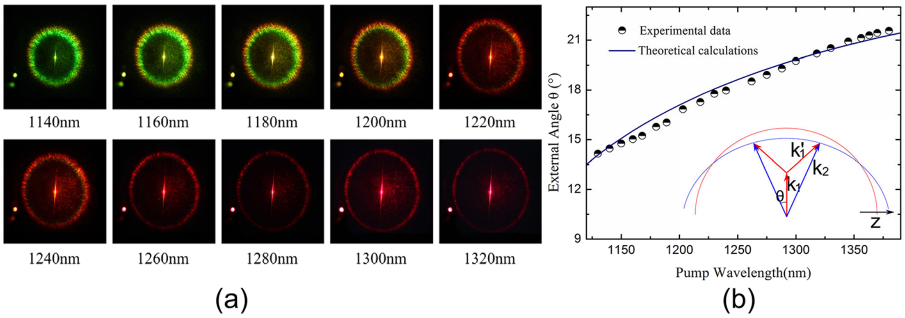

FIG. 1. (a) The conical SHG patterns on the screen by adjusting the pump wavelength from 1140 nm to 1320 nm. (b) The radiation angle θ as a function of the pump wavelength. The inset shows phase-matching diagram of the conical SH beam generation process under anomalous dispersion condition.

refractive-index inhomogeneity on the micro-scale in the crystal bulk. Besides the imperfections on the surface and inside the crystal, impurity ions are the most important scattering sources.[15,16] Thus, a triangle phase-matching relationship could be realized as

$$\vec{k_2} - \vec{k_1} - \vec{k_1'} = 0. \quad (1)$$

Moreover, the 5%/mol MgO:$LiNbO_3$ crystal effectively simulated an anomalous-dispersion-like environment ($2k_{o1} > k_{e2}$); therefore, the triangle phase-matching relationship could be realized in the bulk crystal without additional reciprocal vectors. This explains why the conical SH beams only emerged when the pump was ordinary-polarized.

The radiation angle θ is defined as the half apex angle of the conical SH emission. According to the refractive index ellipsoid, θ satisfies

$$\frac{n_{2e}n_{2o}}{\sqrt{n_{2o}^2\cos^2\theta + n_{2e}^2\sin^2\theta}} = n_{1o}\cos\theta. \quad (2)$$

The curve calculated based on Eq. (2) fits the measured values as shown in Fig. 1(b), which determines that this conical SH originated from the scattering light.

This scheme in anomalous dispersion medium provides possibilities for engineering efficient frequency conversion. By solving the nonlinear wave coupling equation,[17] the SH intensity can be expressed as $I(2\omega) \propto I(\omega)I'(\omega)L^2$, where L^2 is the interaction volume, and $I(\omega)$, $I'(\omega)$ are the intensity of incident light and scattering light, respectively. This formula indicates that the intensity of scattering light restricts the SHG conversion efficiency. But if the scattering light was replaced with a stronger one, the conversion efficiency can be greatly improved. Here, we propose a convenient approach, which takes use of the fundamental frequency component from total reflection inside the crystal, as shown in Fig. 2(a). Under this approach, simply adjusting the direction of incident light, one can produce efficient SH output.

In the experiment, the sample was placed on a rotation stage in its x-z plane, so that the included angle α of incident light and the crystal's x-axis could be adjusted. When the incident light encountered the sidewall, the SH ring was split into two rings which were presented in axial symmetry or mirror symmetry. As the matching relationship in Fig. 2(c) shows, the other ring was originated from the reflected light and scattering light. Due to total reflection within the crystal, a part of the conical SH could not get out from the end face of the sample, so the ring was always incomplete, as shown in Fig. 2(b). From the photos, we also see three symmetrical distributed SH spots. The bilateral points are the collinear SH beams of the incident light and the reflected light, and the central one along the crystal's x-axis is a phase-mismatched sum frequency of them. When increasing the incident angle until the two rings were tangent, the SH intensity at the point of tangency was significantly enhanced. At this time, both $\vec{k_1}$, $\vec{k_1'}$ and $\vec{k}_{1re}$, $\vec{k_1''}$ constitute a triangle phase-matching relation associated with the second harmonic along the x-axis $\vec{k_2}$ as shown in Fig. 2(d), so the scattering light $\vec{k_1'}$ and the reflected light $\vec{k}_{1re}$ were just parallel, and $\vec{k_1'}$ could be replaced by $\vec{k}_{1re}$, which greatly improved the SHG efficiency.

Although the pump has a bandwidth of about 75 nm, the full width at half maximum (FWHM) of phase-matched SH is only 3 nm; in other words, the mechanism is narrowband, which is the same as the BPM and QPM technique. This is because an incident angle only corresponds to a certain phase-matched frequency, which must satisfy $2k_{1o}\cos\alpha = k_{2e}$, i.e.,

$$\alpha = arc\cos(n_{2e}/n_{1o}). \quad (3)$$

For the broadband pump, this phase-matched SH could be obtained in a wide range of incident angles (Fig. 3(a)). Figure 3(b) shows the center wavelength of the phase-matched SH depending on the external incident angle, the results are well consistent with the theoretical prediction.

The conversion efficiency is a key aspect we concentrate on in this experiment. We measured the SHG output power

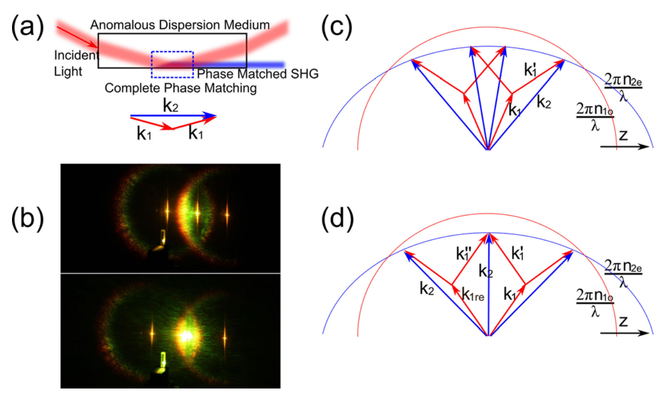

FIG. 2. (a) Scheme of complete phase-matching by total reflection under anomalous dispersion condition. (b) The mirror-symmetrical rings observed with pump pulses at the wavelength of 1190 nm from different incident angles. (c) and (d) Phase-matching diagrams for the general situation of oblique incidence, and the situation that the two SH rings are tangent.

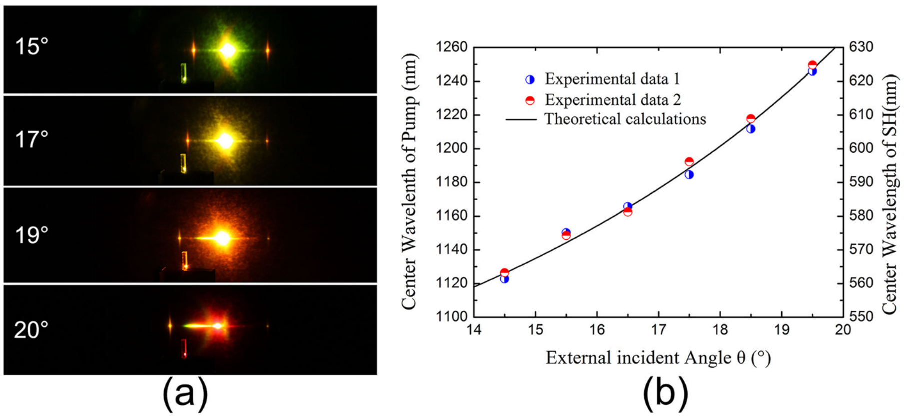

FIG. 3. (a) Photograph of phase-matched SH at the tangent point of two SH rings with the pump from different external incident angles (15°, 17°, 19°, and 20°). (b) The center wavelength of the phase-matched SH depending on the external incident angle. The solid line represents a fit of Eq. (3).

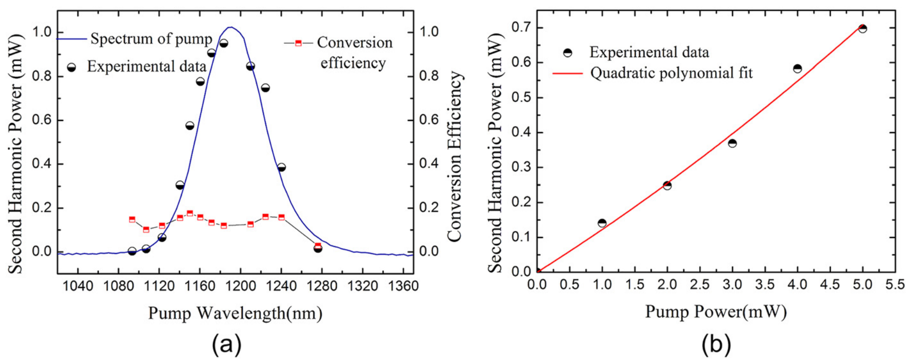

FIG. 4. (a) Measured power of phase-matched SH as a function of the pump wavelength (pump power: 6 mW); the blue solid line represents the experimental spectrum of the pump (arbitrary unit); the red squares are relative conversion efficiency calculated based on the pump spectral information and the SH power. (b) The square law dependence of the SH power on the pump power.

at different incident angles, and according to the relationship of the angles and the matching wavelength (Fig. 3(b)), we obtained the SHG power corresponding to different spectral components of the pump pulse, as shown in Fig. 4(a). Since spectrum of the pump has a Gaussian envelope, the experimentally measured SHG output power also has a similar distribution. Although each frequency component desires different phase matching angle, their conversion efficiency makes little difference. Spectral measurement showed that the actual center wavelength of the pump was at 1190 nm. At the matching angle of center wavelength, we measured SHG output power of 595 nm while changing the energy of the pump by a continuously variable optical attenuator, as shown in Fig. 4(b). Due to instability of the OPA output and the limited adjustable energy range (0–5 mW), the square law dependence of $I(2\omega)$ on $I(\omega)$ is not very clear, but the trend conforms to the theory. The maximum average power we obtained was 0.74 mW at the input power of 5 mW with an efficiency of 14.8%. Considering that such SHG process was realized through a single reflection, and the overlap region of the fundamental wave was only several hundred microns, this was a relatively high conversion efficiency. To increase the nonlinear interaction length, the beam width should be wider, but this also means that the power density is decreased, leading to lower conversion efficiency. Then, another way should be given to further improve the conversion efficiency. For example, by designing appropriate cavity structure, we can make the SH beam generated by multiple reflections coherently superpose. Such a configuration can be implemented in a waveguide structure and an optical resonator, and may be applied in the micro-structural devices.

In conclusion, the specific completely phase-matched conical SH beams can be generated in the bulk anomalous dispersion medium. By the use of this mechanism, we proved that the fundamental frequency component from total reflection inside an anomalous dispersion medium could meet this non-collinear phase-matching condition, and result in efficient frequency doubling. Experimentally, SHG conversion efficiency of a single total reflection was up to 14.8%. Considering the overlapping area of incident light and reflected light is small, this frequency doubling process actually has very high conversion efficiency, which is with great potential for practical applications.

This work was supported in part by the National Basic Research Program "973" of China under Grant No. 2011CB808101, the National Natural Science Foundation of China under Grant Nos. 61125503, 61235009, and 61205110, the Foundation for Development of Science and Technology of Shanghai under Grant No. 11XD1402600, and in part by the Innovative Foundation of Laser Fusion Research Center.

[1]J. A. Armstrong, N. Bloembergen, J. Ducuing, and P. S. Pershan, Phys. Rev. **127**(6), 1918–1939 (1962).
[2]P. Xu, S. Ji, S. Zhu, X. Yu, J. Sun, H. Wang, J. He, Y. Zhu, and N. Ming, Phys. Rev. Lett. **93**(13), 133904 (2004).
[3]H. Huang, C. P. Huang, C. Zhang, D. Zhu, X. H. Hong, J. Lu, J. Jiang, Q. J. Wang, and Y. Y. Zhu, Appl. Phys. Lett. **100**(2), 022905 (2012).
[4]Z. Xie, G. Zhao, P. Xu, Z. Gao, and S. Zhu, J. Appl. Phys. **101**(5), 056104 (2007).
[5]Y. Zhang, Z. D. Gao, Z. Qi, S. N. Zhu, and N. B. Ming, Phys. Rev. Lett. **100**(16), 163904 (2008).

[6]A. Fragemann, V. Pasiskevicius, and F. Laurell, Appl. Phys. Lett. **85**(3), 375–377 (2004).
[7]N. An, H. J. Ren, Y. L. Zheng, X. W. Deng, and X. F. Chen, Appl. Phys. Lett. **100**(22), 221103 (2012).
[8]Y. Sheng, V. Roppo, Q. Kong, K. Kalinowski, Q. Wang, C. Cojocaru, J. Trull, and W. Krolikowski, Opt. Lett. **36**(13), 2593–2595 (2011).
[9]A. S. Aleksandrovsky, A. M. Vyunishev, A. I. Zaitsev, A. A. Ikonnikov, and G. I. Pospelov, Appl. Phys. Lett. **98**(6), 061104 (2011).
[10]X. Deng and X. Chen, Opt. Express **18**(13), 15597–15602 (2010).
[11]H. Ren, X. Deng, Y. Zheng, N. An, and X. Chen, Phys. Rev. Lett. **108**(22), 223901 (2012).
[12]O. Gayer, Z. Sacks, E. Galun, and A. Arie, Appl. Phys. B: Lasers Opt. **91**(2), 343–348 (2008).
[13]J. Giordmaine, Phys. Rev. Lett. **8**(1), 19–20 (1962).
[14]Y. Chen, K. Su, T. Lu, and K. Huang, Phys. Rev. Lett. **96**(3), 033905 (2006).
[15]K. Bastwöste, U. Sander, and M. Imlau, J. Phys.: Condens. Matter **19**(15), 156225 (2007).
[16]Y. Ja, J. Opt. **21**(1), 41 (1990).
[17]R. W. Boyd, *Nonlinear Optics*, 2nd ed. (Academic Press, San Diego, CA, 2003).